TYPE Original Research
PUBLISHED 29 September 2025
DOI 10.3389/fbuil.2025.1670013



OPEN ACCESS

EDITED BY Yan Li,

Nanyang Normal University, China

REVIEWED BY

Xiuze Fan, Washington State University, United States Zhichao Huang, Southwest Jiaotong University, China

*CORRESPONDENCE

Yanan Zhao, ⋈ 18236850373@163.com

RECEIVED 22 July 2025 ACCEPTED 25 August 2025 PUBLISHED 29 September 2025

CITATION

Zhang M, Zhao Y, Wang C, Jin D and Chen Q (2025) Research on the pavement performance of lignin fiber toughened foam asphalt cold recycled mixes. Front. Built Environ. 11:1670013. doi: 10.3389/fbuil.2025.1670013

COPYRIGHT

© 2025 Zhang, Zhao, Wang, Jin and Chen. This is an open-access article distributed under the terms of the Creative Commons Attribution License (CC BY). The use, distribution or reproduction in other forums is permitted, provided the original author(s) and the copyright owner(s) are credited and that the original publication in this journal is cited, in accordance with accepted academic practice. No use, distribution or reproduction is permitted which does not comply with these terms

Research on the pavement performance of lignin fiber toughened foam asphalt cold recycled mixes

Min Zhang¹, Yanan Zhao²*, Chenxi Wang², Duo Jin¹ and Qi Chen²

¹China Railway Fifth Bureau Group Mechanized Engineering Company Limited, Hengyang, Hunan, China, ²National Key Laboratory of Green and Long-Life Road Engineering in Extreme Environment, National Engineering Research Center of Highway Maintenance Technology, School of Transportation, Changsha University of Science and Technology, Changsha, China

To improve the pavement performance and toughness of foam asphalt cold recycled mixture (FACRM), the effects of lignin fiber on the pavement performance of FACRM at 0%, 0.3%, 0.6% and 0.9% dosages (relative to foam asphalt cold recycled mixtures) were investigated. The influence of different fiber dosages on the performance of FACRM was investigated through the high-temperature rutting, semi-circular bending, and freeze-thaw splitting tests, and the microscopic morphology of the fiber on the FACRM damage interface was observed by scanning electron microscope (SEM). The results show that with the increase in lignin fiber dosage, the maximum dry density of FACRM shows a decreasing trend; the optimum moisture content and the optimum asphalt content gradually increase; dynamic stability, fracture energy, and tensile strength ratio (TSR) show a pattern of change that first increases and then decreases. The fiber enhancement mechanism of FACRM pavement performance is that its dispersion as a bridge in the mixture to form a threedimensional network structure provides the reinforcement. The recommended dosage is 0.3% based on a comprehensive review of the effects of lignin fiber on the recycled mixture pavement performance and microscopic morphology of the results.

KEYWORDS

cold recycled asphalt mixtures, foam asphalt, pavement performance, lignin fiber, reinforcement

1 Introduction

Foam asphalt is a temporarily expanded state material formed by injecting a small amount of cold water into hot asphalt, which combines high specific surface area and low viscosity characteristics (Li et al., 2024). It has a wide range of applications in the field of cold pavement rejuvenation and sustainable road construction. However, foam asphalt cold recycled mixture (FACRM) has toughness problems, such as low early strength (Li et al., 2016), poor durability, and weak high-temperature stability due to slow bonding caused by room temperature construction, insufficient fusion of reclaimed asphalt pavement (RAP) and new asphalt, and thin and uneven distribution of foam asphalt film (Song et al., 2024a). Many researchers have studied and found a variety of technical paths to enhance the

toughness of FACRM. Thermoplastic resins, polymer, rubber, rejuvenating agents, and other modifiers can improve the toughness by improving the interfacial cohesion (Song et al., 2024a; Hu et al., 2024; Song et al., 2024b; Algraiti and Kavussi, 2023), and epoxy resin can improve the performance by forming a highly viscous thermosetting slurry and "embedded" asphalt molecules (Chen et al., 2025). During the addition of mineral admixtures, cement and other mineral admixtures form a spatial three-dimensional grid structure to play a reinforcing role (Li et al., 2019), significantly enhancing the overall stability of the foam asphalt mortar. In terms of raw material control, controlling the aging degree and dosage of RAP material can reduce the influence of unfavorable factors (Ai et al., 2025; He and Wong, 2008). Research has confirmed that fiber can effectively enhance the pavement performance of mixtures. In terms of low-temperature crack resistance, lignin fiber has a significantly better effect than glass fiber (Luo et al., 2019). Existing research has shown that lignin fiber can improve the high-temperature stability of hot-mix asphalt mortar and modified asphalt concrete (Pang et al., 2023; Fazilah et al., 2025; Yue et al., 2022). In terms of cost-effectiveness, lignin fiber shows significant advantages. The raw material cost of lignin fiber is only 1/3 to 1/5 of that of petroleum-based synthetic fiber, and the price range for conventional lignin fiber is \$0.9/kg, compared to \$2/kg for comparable synthetic fiber, which gives it a very good economic advantage. Existing research has mainly focused on the pavement performance of fiber-reinforced asphalt mixtures and hot recycled asphalt mixtures (Nian et al., 2024; Fei et al., 2025). However, there are few systematic studies on the effect of fibers on the pavement performance of FACRM in existing studies.

Based on this, this study introduces lignin fiber into a FACRM system, determines the optimum asphalt content, maximum dry density, and optimum moisture content under different fiber dosage through wet and dry splitting test and compaction test, explores the improvement law of fiber dosage on pavement performance of mixes based on the tests of high-temperature rutting, semi-circular bending, and freeze-thaw splitting tests, and analyzes the effect of fiber on the fine microscopic morphology of the damage interface through SEM. The article then puts forward the recommended dosage for engineering applications and provides a theoretical basis and technical support for the popularization and application of foam asphalt cold recycled technology.

2 Materials and methods

2.1 Experimental materials

2.1.1 Reclaimed asphalt pavement (RAP)

The RAP used in the study was taken from the sixth contract section of the reconstruction and expansion project of the Suizhong-Panjin section of the Beijing-Harbin Expressway in Liaoning Province and classified as Grade 2 RAP. The RAP was derived from the old pavement milling material, which was crushed and screened (dry sieving method) into three grades of aggregates: 0–5 mm, 5–10 mm, and 10–20 mm, as shown in Table 1.

2.1.2 New aggregates

The new aggregates used in the study include 20–30-mm coarse aggregate, 0–3-mm fine aggregate, and mineral powder. Their technical indexes are in line with the requirements of the Technical Specification for the Construction of Highway Asphalt Pavements (JTG F40-2004-T0316), which were obtained by sieving the various grades of aggregates by using the water sieving method. The sieving results are shown in Table 2.

2.1.3 Bitumen foam

The original asphalt used in the foam asphalt preparation process was No. 90 Grade A road petroleum asphalt produced by China Foshan Gaofu PetroChina Company. The foaming temperature was 155 °C–160 °C, the foaming water consumption was 2.0%, and the final prepared foam asphalt had an expansion rate of $10.5 \times$ and a half-life of 16 s.

2.1.4 Lignin fiber

The test used lignin fiber produced by Shandong Road New Road Maintenance Materials Co., Ltd. In view of the threedimensional network structure of lignin fiber, which can effectively adsorb asphalt to prevent asphalt segregation of the mixture, the special length-to-diameter ratio can optimize the stress transfer to effectively improve the low-temperature crack resistance and rutting resistance of the mixture, taking into account the economy and environmental protection, and is widely used in engineering practice. Therefore, lignin fiber was selected as the pavement performance toughening agent of FACRM in this study, and the related technical indexes are shown in Table 3. Fiber dosages were selected based on an extensive literature review (Wang et al., 2025; Luo et al., 2019; Hui et al., 2022; Anurag et al., 2009; Alfalah et al., 2021), indicating 0.3%-0.9% as the optimal range for FACRM. The mass fractions of fiber blending were 0%, 0.3%, 0.6%, and 0.9% (relative to the mass of FACRM), and the blending method was external blending.

2.1.5 Cement

This study used ordinary Portland cement produced by China Resources Cement Limited, with a cement strength class of 32.5. The cement was added externally at a dosage of 1.5% (relative to the total mass of the aggregate). The cement was in a loose, dry state, free of lumps, and had not deteriorated due to moisture.

2.2 Aggregate gradation design

Based on the screening results of RAP and new aggregate of various grades, an AC-25 gradation design was developed. After adjustment, the ratio of RAP 10–20 mm:RAP 5–10 mm:RAP 0–5 mm:20–30 mm:0–3 mm:mineral powder was determined to be 21:22:28:15:10:4. The final aggregate gradation results are shown in Table 4. The relevant Marshall volume parameter indicators are shown in Table 5 and meet the specifications.

TABLE 1 RAP sieving results for each grade of aggregate.

Aggregate specification		Percentage of passage through different sieve holes (mm)/%											
	31.5	26.5	19	16	13.2	9.5	4.75	2.36	1.18	0.6	0.3	0.15	0.075
RAP 10–20 mm	100	100	79.3	49.6	19.6	1.3	0.4	0.4	0.4	0.4	0.4	0.4	0.1
RAP 5–10 mm	100	100	100	100	97.0	45.6	0.7	0.7	0.7	0.7	0.7	0.7	0.3
RAP 0–5 mm	100	100	100	100	100	100	83.1	54.9	39.8	22.3	11.3	6.2	2.9

TABLE 2 Sieving results for each grade of new aggregates.

Aggregate specification		Percentage of passage through different sieve holes (mm)/%											
	31.5	26.5	19	16	13.2	9.5	4.75	2.36	1.18	0.6	0.3	0.15	0.075
20–30 mm	100	73.0	2.4	0.2	0.2	0.2	0.2	0.2	0.2	0.2	0.2	0.2	0.2
0–3 mm	100	100	100	100	100	100	99.2	65.1	44.4	24.9	15.6	11.7	9.5
Mineral powder	100	100	100	100	100	100	100	100	100	100	97.8	91.2	79.4

TABLE 3 Lignin fiber specifications.

Performance indicator	Length	Ash content	рН	Moisture content
Lignin fiber	≤6 mm	18%	7.5	4%

3 Test methods

3.1 Physical parameter test

Three-layer specimens with different moisture contents (6.4%, 6.6%, 6.8%, and 7%) were prepared by the heavy-duty compaction method, and the maximum dry density and optimum moisture content were determined by measuring the relationship curve between dry density and moisture content. In addition, Marshall specimens with different foam asphalt dosages (2.8%, 3.0%, 3.2%, 3.2%, and 3.6%) were produced, and the dry and wet split strengths of the specimens after freeze-thaw cycles were tested by referring to the "Test Procedure for Asphalt and Asphalt Mixtures for Highway Engineering" (JTG E20-2011-T0729) (hereinafter referred to as the Standards) and calculating the tensile strength ratio (TSR) to determine the optimum asphalt content.

3.2 High-temperature rutting

According to Standard (2011-T0703), milling molding length 300 mm, width 300 mm, thickness 50 mm, rutting plate, and to Standard (2011-T0719), rutting test to evaluate the high-temperature performance of cold recycled mixtures, the test temperature was $60\,^{\circ}\text{C}$, and the wheel pressure was $0.7\,\text{MPa}$.

3.3 Semi-circular bending test

Semi-circular bending specimens were made by cutting the middle 50 mm thickness portion of a 150 mm diameter Marshall specimen, and cutting a 15 mm precast seam at the bottom center after cutting the specimen in half along the diameter (Meng et al., 2023). Before the test, the test piece was placed in a constant temperature chamber at $-10~^{\circ}$ C, and the temperature was controlled for 4 h. Then, the low-temperature crack resistance of FACRM was evaluated by performing the low-temperature semi-circular bending test (loading rate 50 mm/min, $-10~^{\circ}$ C) according to the "American Association of State Highway and Transportation Officials" (TP105).

3.4 Freeze-thaw splitting test

The Material Testing System (MTS) testing machine was used for loading and testing to determine the change rule of force–displacement at the bottom of the specimen during the loading process, according to the Standard (2011-T0729). The large Marshall specimen was divided into two groups. One group was reserved, and the other group was first kept in a vacuum for 15 min and then kept at atmospheric pressure for 0.5 h. Then, the specimen was put into a plastic bag with 10 mL of water and taken out of the plastic bag after the sample had been frozen for 16 h at $-20\,^{\circ}\mathrm{C}$.

3.5 Scanning electron microscope (SEM)

A Hitachi S-340N SEM with nanometer resolution was employed to characterize surface morphology, microstructural features, particle distribution, and defects in asphalt and asphalt mixtures using secondary electron detection.

TABLE 4 Aggregate gradation.

Aggregate specifications	Percentage of passage through different sieve holes (mm)/%												
	31.5	26.5	19	16	13.2	9.5	4.75	2.36	1.18	0.6	0.3	0.15	0.075
Determination of gradation	100	95.9	81	74.5	67.5	52.3	37.4	26.1	19.8	13.0	8.9	6.8	5.1

TABLE 5 Marshall volume parameter indicators.

Parameter	Experimental results	Regulatory requirements
Air voids (AV/VV)	5.3%	4%-6%
Voids in mineral aggregate (VMA)	14.7%	>14%
Voids filled with asphalt (VFA)	67.0%	65%-75%

4 Results and discussion

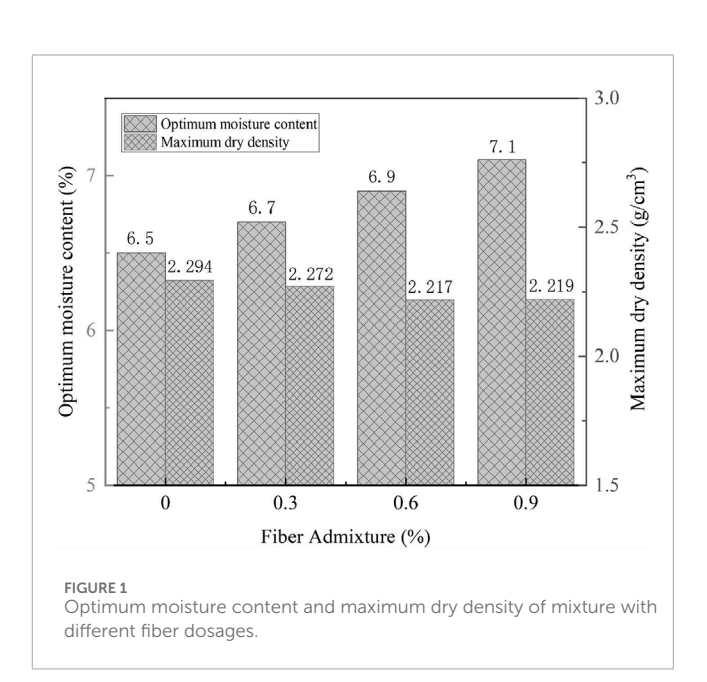
4.1 Maximum dry density, optimum moisture content, and optimum asphalt content

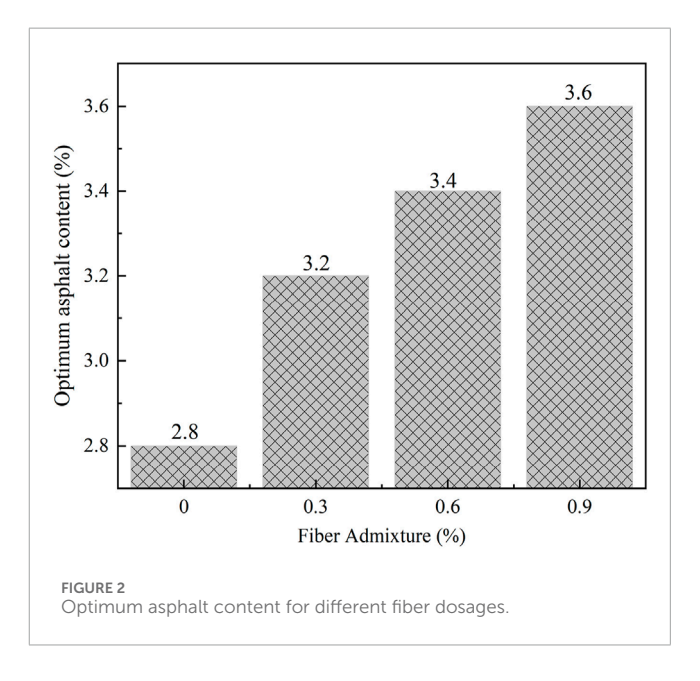
4.1.1 Maximum dry density and optimum moisture content

Figure 1 shows the results of optimum moisture content and maximum dry density of mixes with different fiber dosages. As shown in the figure, with the increase of fiber doping, the maximum dry density first decreases from 2.294 g/cm3 to 2.217 g/cm3 and then tends to level off, and the optimum moisture content linearly increases from 6.5% to 7.1%. This is mainly because the lignin fiber density (0.4-0.7 g/cm³) is much lower than the density of the mineral material (2.6-2.9 g/cm³). After mixing, an equivalent volume has a decreased dry density. At the same time, the fiber contains hydroxyl, carboxyl, and other hydrophilic groups and can be adsorbed with water molecules to form a large number of hydrogen bonds, so that the moisture content increases. In addition to the surface roughness of the fiber, the adsorption optimized distribution of the cement phase and promoted asphalt to fully fill the mineral material (Ren et al., 2022). It can optimize the distribution of the cementing phase and promote the asphalt to fill the gaps in the mineral material.

4.1.2 Optimum asphalt content

Figure 2 demonstrates the optimum asphalt content for FACRM with different fiber dosages. As shown in the figure, the optimum asphalt content of FACRM increases with the increase of fiber dosage (from 2.8% to 3.6%), which is due to the fact that the fiber, as a special filler, must be encapsulated by asphalt, and its incorporation increases the specific surface area of the mix (Shi et al., 2023). More asphalt must be adsorbed in order to obtain the best cracking resistance. When the fiber dosage exceeds 0.3%, the optimum asphalt content growth rate is significantly reduced, because the fiber





dosage is lower than can be uniformly dispersed. Meanwhile, a fiber dosage of more than 0.3% is prone to agglomeration, resulting in a reduction in the effective adsorption at the interface and a decrease in the macro-performance of the asphalt consumption.

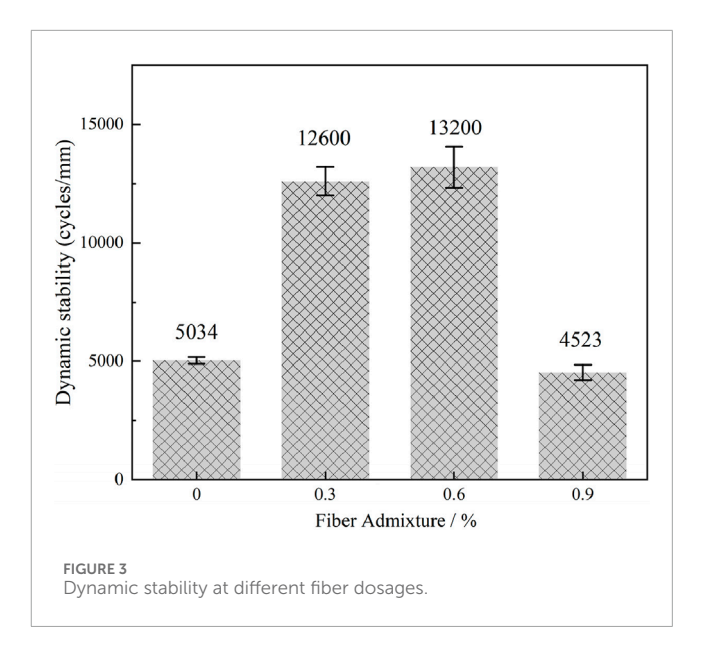
4.2 Effect of fiber incorporation on pavement performance of cold recycled mixes

4.2.1 High-temperature stability

Figure 3 shows the dynamic stability of the mixtures under different fiber dosages. The dynamic stability of FACRM shows a tendency to increase from 5,034 cycles/mm to 13,200 cycles/mm and then decrease from 13,200 cycles/mm to 4,523 cycles/mm with the increase of fiber dosage. It reaches the maximum value at 0.6% dosage, and the dynamic stability at the 0.3%, 0.6%, and 0.9% dosages is 2.5 times, 2.61 times, and 0.9 times of the original value, respectively, which indicates that the moderate amount of fiber dosage can significantly improve the high-temperature stability of the mixture, and an excessive dosage can negatively affect stability. This is because the appropriate amount of lignin fibers can form a three-dimensional mesh structure in the mixture to produce a reinforcing effect, and adsorption of asphalt increases the thickness of the structural film, effectively resisting hightemperature deformation (Wu et al., 2022; Shi et al., 2023). However, excessive fiber content (0.9%) tends to clump and aggregate during mixing, forming localized weak interface zones that hinder uniform asphalt coating of aggregates and weaken interlocking forces between aggregates; lignin fibers have an oil absorption rate of approximately 1-2 times their own weight. At a dosage of 0.9%, excess fibers competitively adsorb asphalt (especially aged components in recycled asphalt), leading to a reduction in effective asphalt film thickness, decreased lubricity of the mixture, and exacerbated high-temperature shear deformation. Additionally, when the fiber content exceeds 0.6%, excess fibers form a noncontinuous network structure in the mixture, disrupting the density of the mineral aggregate skeleton, reducing the probability of direct contact between aggregates, weakening the friction effect, and causing a decrease in high-temperature stability (Liu et al., 2023). Therefore, when considering only the high-temperature stability performance of FACRM, the recommended fiber content is 0.3% and 0.6%.

4.2.2 Low-temperature crack resistance

Figure 4a shows the typical load-displacement curve schematic of the mix, and Figure 4b shows the stress-strain curves under different fiber dosages. As shown in the figure, with the increase of the fiber dosage, the peak load and the load area of the FACRM show the characteristics of the change of the first increasing and then decreasing, which indicates that the dosage of an appropriate amount of fibers can enhance the ability of FACRM to resist crack generation and delay crack extension. The possible reasons for this are: first, lignin fibers have high ductility, forming a threedimensional network structure in the mixture, which improves the overall toughness of the material (Kong et al., 2022; Luo et al., 2019). Second, the physical adsorption and chemical bonding between the fibers and asphalt enhances the interfacial bonding force; when the temperature is lowered, such a network structure can effectively impede microcracks from sprouting and dispersing the stress concentration, and at the same time, inhibit the expansion of cracks (Kong et al., 2022; Luo et al., 2019), improve crack resistance and delay crack extension ability of FACRM, improving the cracking toughness of the mixture. However, when the fiber doping exceeds



0.6%, its dispersion uniformity decreases, and it easily forms agglomerates, which trigger local stress concentration around the clusters and produce microcracks, which accelerate the expansion under low-temperature conditions and significantly weaken the low-temperature crack resistance of the mixture (Akram et al., 2024).

As shown in Table 6, the five indices of FACRM show the trend of increasing and then decreasing with the increase of fiber dosage. This is because an appropriate amount of lignin fiber forms a continuous three-dimensional network structure by adsorbing asphalt, which effectively transmits load stress and disperses crack propagation energy; at the same time, plastic deformation occurs at the fiber-asphalt interface, absorbing crack propagation energy and reducing the stress concentration factor; Furthermore, the high oil absorption rate of lignin fiber retains sufficient free asphalt to coat the aggregate, maintaining the flexibility of the mixture. The rigid framework of the fiber complements the viscoelastic properties of the asphalt to improve the crack resistance of the mixture. Considering the comprehensive effects of lignin fiber on asphalt mixture low-temperature performance characteristics, it is recommended that engineering applications of lignin fiber use a dosage of 0.3%.

4.2.3 Moisture susceptibility

Figure 5 shows that lignin fiber has a significant effect on the moisture susceptibility of cold recycled mixes. The split strength and residual strength ratio (TSR) both show a trend of first increasing and then decreasing. The split strength reaches the maximum value (0.54 MPa) at 0.3% doping, which is higher than that of the benchmark group (0.48 MPa), and still maintains the highest strength after freeze-thawing (0.44 MPa). However, the effect of the increase in TSR is not significant (only 12.5%). The TSR values decreased to 92% and 60% of the unadulterated fibers, respectively, which is due to the strong water absorption of lignin fiber, leading to an increase in the water absorption rate of the mix. The freezing and thawing cycle produces volumetric expansion stress to weaken the interfacial bond strength. High dosages tend to agglomerate the formation of the local weak areas (Zarei et al., 2022; Wang et al.,

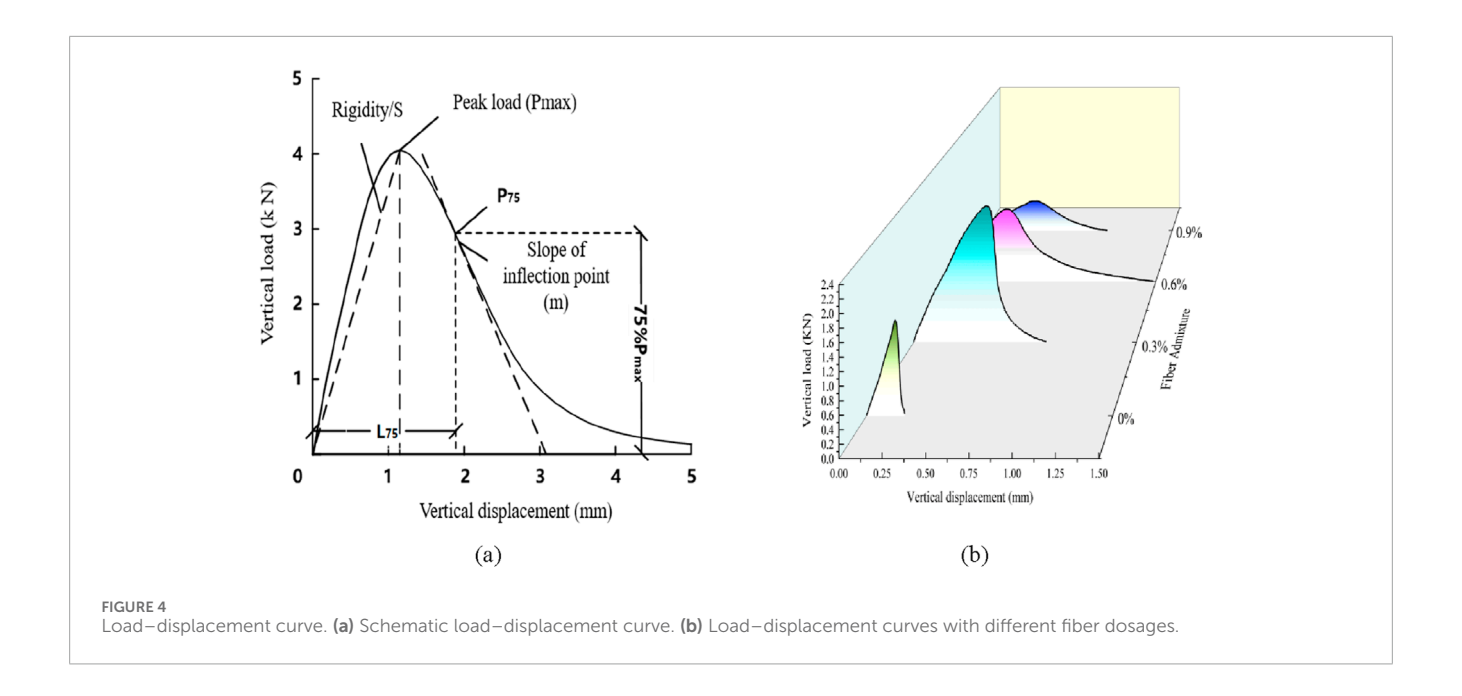


TABLE 6 Effect of fiber dosage on low-temperature crack resistance of cold recycled mixes.

Relevant indicator	Lignin fiber content							
	0	0.3%	0.6%	0.9%				
Fracture energy G _f (J/m ²)	51.86	222.05	202.65	67.64				
Peak load (kN)	1.53	2.33	1.13	0.43				
Cracking resistance index (mm ⁻¹)	33.89	101.16	173.99	156.24				
Peak-to-peak load area (kN⋅m)	0.1159	0.6326	0.3020	0.1322				
Post-peak load area (kN·m)	0.0379	0.2068	0.3690	0.1363				

2024). Therefore, it is recommended that the fiber dosage in engineering applications is 0.3%.

4.3 Effect of fiber incorporation on the microscopic morphology of the damage interface of cold recycled mixtures

An SEM examination was used to reveal the effect of fiber doping on the microscopic morphology of the FACRM damage interface. The fracture damage interfaces of the various samples, including RAP, the undoped fiber mixture, the 0.3% fiber-doped mixture, and the 0.6% and 0.9% fiber-doped mixtures, respectively, were examined, and the specific results are as follows:

4.3.1 RAP

The RAP was taken from the old asphalt pavement of the sixth contract section of the reconstruction and expansion project of the Suizhong-Panjin section of the Beijing-Harbin Expressway in Liaoning Province and classified as Grade 2 RAP. Figure 6 shows

the microscopic morphology of the RAP under magnifications of $\times 500, \times 1000,$ and $\times 2000.$ As shown in the figure, asphalt pavement exposed to vehicle load and environmental factors forms many wrinkle-like raised structures. Its size distribution and molecular chain crosslinking degree are closely related. The local area can be seen in bright white spots, which accounted for approximately $8\% \sim 12\%$ of the total area. These spots may be some of the components in the asphalt oxidation, aggregation, and other reactions in the aging process. The formation of some of the asphalt and the nature of different substances experience different microcosms. These spots may be the oxidation of some components in the asphalt during the aging process, forming some substances with different properties from the surrounding asphalt, which show a bright white color under microscopic observation.

4.3.2 FACRM without fiber

As shown in Figure 7, compared with the RAP in Figure 6, after adding foam asphalt, the aggregate surface of RAP material is encased in a thinner and more uniform film, and there are a few traces of air bubbles at the interface between asphalt and aggregate and inside the asphalt film. These residual traces show some round or oval tiny cavities, which are the water vapor escape residues during the foaming process. Due to the good wettability and adhesion of the foam asphalt, the thickness of the interfacial transition zone is reduced, which is significantly improved compared with the aged asphalt interface (Li et al., 2024; Bairgi et al., 2019). Further observation shows that the boundary between the asphalt and the aggregate becomes fuzzy, and more asphalt molecules are physically or chemically adsorbed onto the minerals on the aggregate surface. The asphalt evaporation residual phase forms a honeycomb continuous network structure with a certain void ratio. No fiber-reinforcing phase exists, and its strength is completely dependent on the asphalt-aggregate interfacial adhesion.

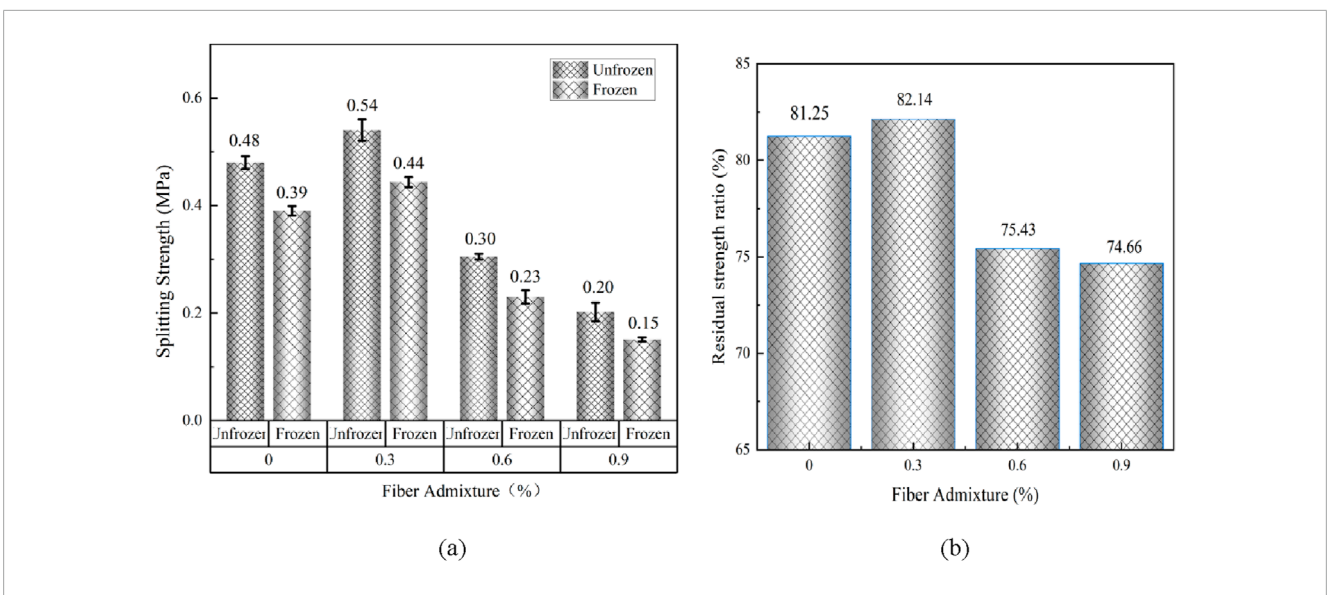
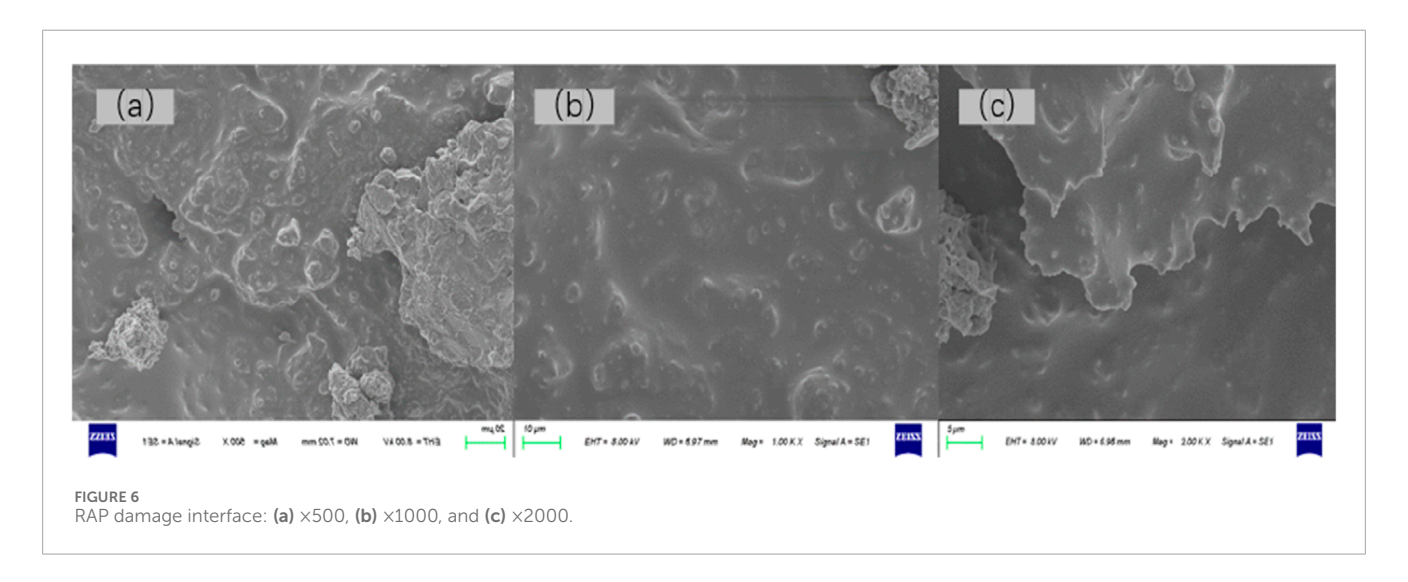


FIGURE 5
Splitting strength vs residual strength ratio for different fiber dosages. (a) Freeze-thaw and unfreeze-thaw splitting strengths. (b) Residual strength ratio of mixes with different fiber dosages.



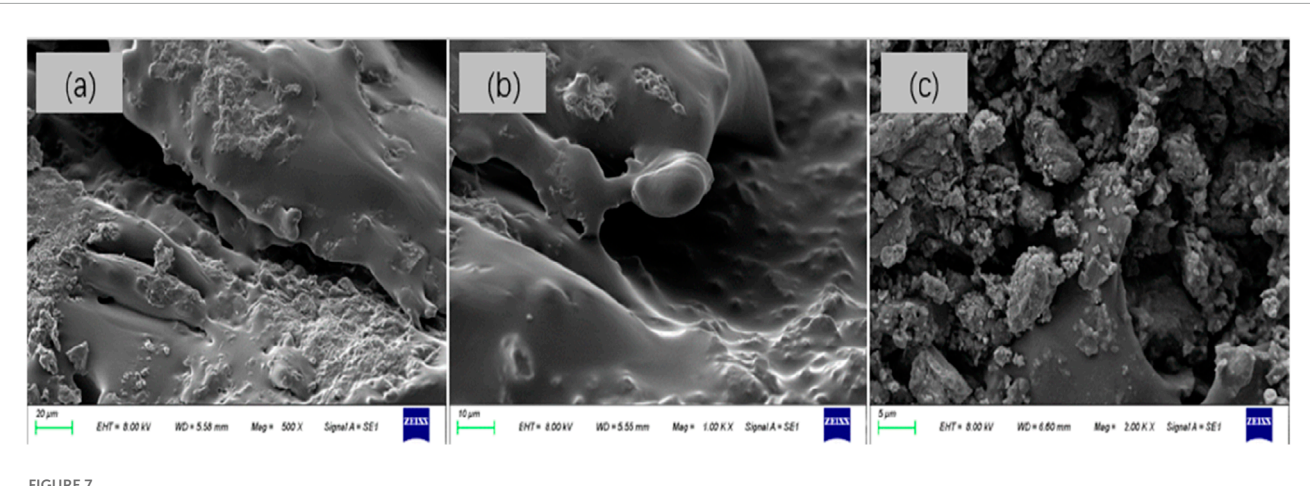
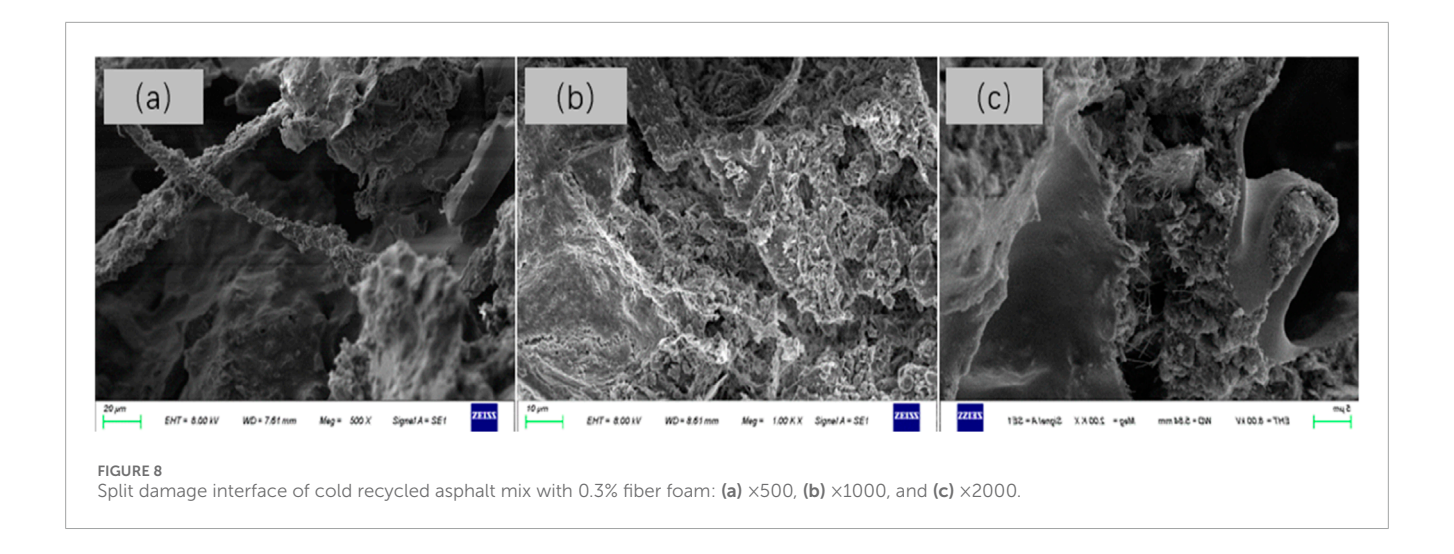


FIGURE 7
Split damage interface of cold recycled asphalt mixes without fiber foam: (a) ×500, (b) ×1000, and (c) ×2000.



4.3.3 FACRM with 0.3% fiber

Figure 8 shows the microscopic morphology of the foam asphalt cold recycled mixture with 0.3% fiber under ×500, ×1000, and ×2000 magnification. The sample presented the following characteristics: the lignin fiber in the foam asphalt mixture inside the local formation of a penetrating structure was uniformly dispersed. The fibers overlap each other to form a three-dimensional network structure that serves as a "skeleton" to limit the displacement of asphalt and aggregates to play a reinforcing role (Li et al., 2022). The lignin fiber varied. Long fibers produced a mechanical interlocking effect. The relatively low 0.3% fiber doping is relatively small, and long fibers in the asphalt can be uniformly dispersed to form a wider range of network structures, thereby significantly improving the asphalt's strength, toughness, and resistance to deformation. The enhancement effect is more obvious. Short fibers in asphalt are relatively small and do not easily entangle with each other. Under the action of mixing, the short fibers can be uniformly dispersed in the asphalt system and can improve the strength of the asphalt to a certain extent (Lin et al., 2010), but due to length limitations, the enhancement effect is not as significant as that of the long fibers.

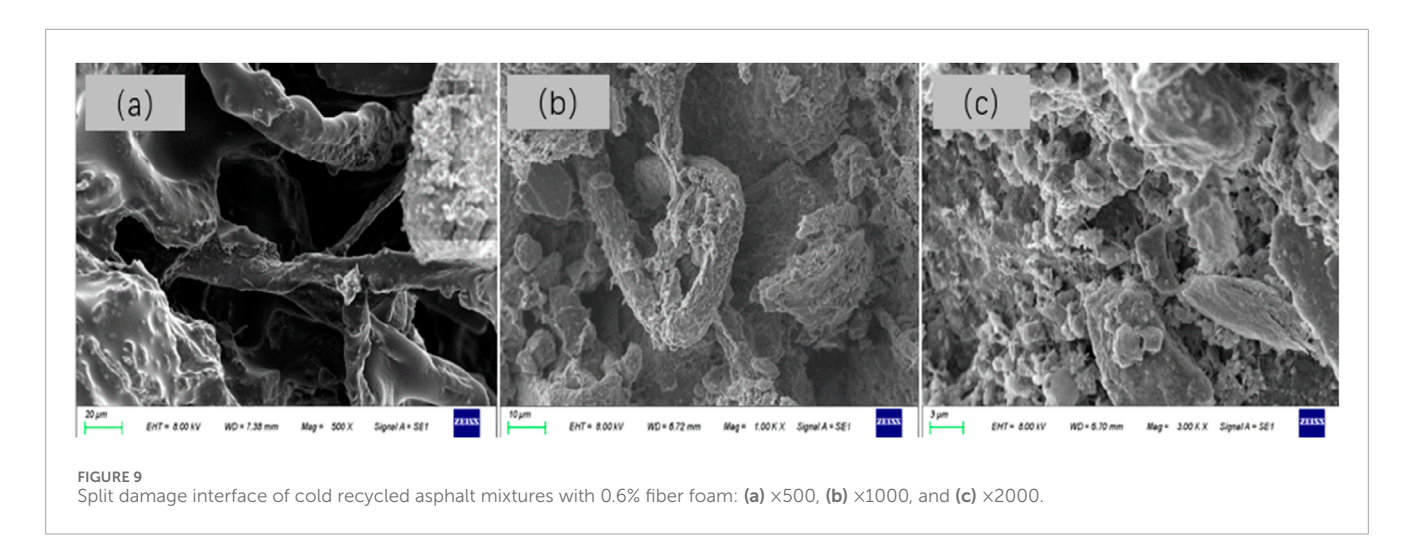
4.3.4 FACRM with 0.6% and 0.9% fibers

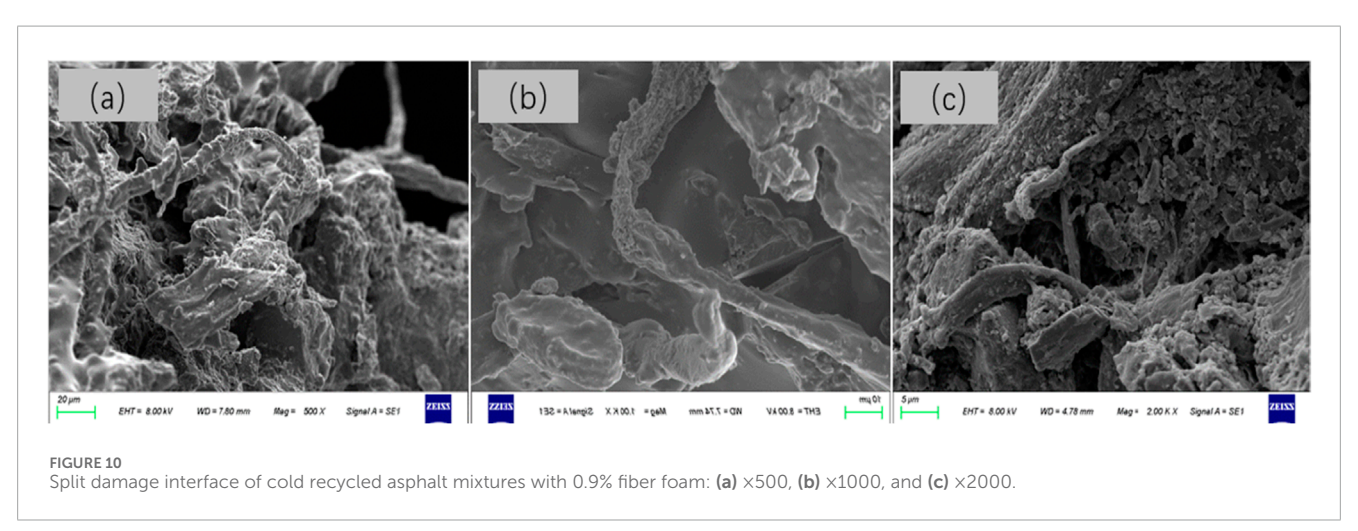
When the fiber content is 0.6% (Figure 9), a three-dimensional network structure has already formed, but the uniformity of fiber dispersion decreases, with slight bundle-like aggregation occurring in some areas. A small number of fibers are inadequately wrapped, resulting in micro-voids at the interface with asphalt. The mechanical properties are still superior to those of the fiberfree group, but the overall performance is lower than that of the optimal fiber content of 0.3%. Fiber doping at 0.9% (Figure 10) is the most significant. Asphalt adsorption increased significantly, and the aggregate surface asphalt film thickness is abnormally thick. Asphalt film that is too thick is not only a waste of material, but also, at high temperatures, it is prone to flow, flooding oil, and other problems, affecting the smoothness and performance of the pavement (Gong et al., 2025; Sengoz and Agar, 2007). Too many fibers entangled with other fibers can disrupt the continuity of the asphalt film. When the mixture is stressed, the discontinuous asphalt membrane cannot effectively transfer the stress. Such a mixture readily concentrates stress in the weak parts, thus reducing the overall strength of the mixture. In addition, when the fiber doping is too high, the fibers compete with each other for the asphalt, resulting in some of the fibers not being adequately wetted by the asphalt and bonding, thereby weakening the interfacial adhesion between the fiber and the asphalt (Wu et al., 2015). Further observation found that too much fiber in the aggregate surface formed a thick layer of fiber, hindering the direct contact between asphalt and aggregate, reducing the bond strength between the aggregate and asphalt interface. Excessive fiber will also form a too dense and complex network structure. This network structure is too rigid and lacks sufficient flexibility and adaptability. When the mixture is impacted by water flow, the network structure is too disordered to work together effectively and is unable to disperse the load uniformly, inducing asphalt film spalling.

5 Conclusion

In this article, the influence of different dosages of lignin fiber on FACRM pavement performance and the microscopic morphology of recycled mixes was investigated. The main findings and conclusions are as follows:

- The high-temperature stability of FACRM showed a significant increase and decrease with the increase of lignin fiber doping.
 The dynamic stability was increased by 150% and 162% at 0.3% and 0.6% fiber doping compared to the undoped sample.
- The low-temperature crack resistance of FACRM showed a tendency to increase and then decrease with the increase in lignin fiber dosages, and the resistance at fiber dosages of 0.6% and 0.9% was only 74% and 28% of the samples without fiber. Fiber doping of 0.3% can increase the fracture energy by 328%, the peak load by 52%, and the cracking resistance index by 200%.
- The moisture susceptibility of FACRM with the increase of lignin fiber doping showed a trend of increasing and then decreasing, and the growth effect is not significant. The moisture susceptibility of FACRM at the optimal doping rate of 0.3% is only 1.01 times that of the recycled mixes without fiber.





However, too high a dosage will have a large negative impact on the moisture susceptibility of the mixture.

• The addition of foam asphalt allows asphalt to cover the surface of RAP aggregate with a thinner and more uniform film. Lignin fiber in the mixture provides uniform internal dispersion, mutual overlap, and the formation of a three-dimensional, mesh-reinforced structure. Too much fiber breaks the continuity of the original asphalt film, resulting in a decline in pavement performance of the asphalt mixtures. The recommended lignin fiber dosage is 0.3%.

6 Future research recommendations

Study will address the mechanism of aging asphalt, foam asphalt, and fiber to establish a quantitative composition–structure–interface model. A different study will introduce digital image correlation (DIC) to track the crack evolution process, combined with the viscoelastic finite element model to establish the rut depth prediction model and the fatigue damage accumulation criterion.

Data availability statement

The original contributions presented in the study are included in the article/supplementary material, further inquiries can be directed to the corresponding author.

Author contributions

MZ: Conceptualization, Funding acquisition, Project administration, Writing – original draft. YZ: Investigation, Methodology, Validation, Visualization, Writing – review and editing. CW: Writing – review and editing, Formal analysis, Methodology. DJ: Writing – review and editing, Funding acquisition, Project administration. QC: Investigation, Writing – review and editing, Formal analysis, Visualization.

Funding

The author(s) declare that financial support was received for the research and/or publication of this article. This work was supported

by the China Railway Fifth Bureau Group Mechanized Engineering Co. (Grant 2024-Key project-14).

Acknowledgments

The authors gratefully acknowledge their financial support.

Conflict of interest

Authors MZ and DJ were employed by China Railway Fifth Bureau Group Mechanized Engineering Company Limited.

The remaining authors declare that the research was conducted in the absence of any commercial or financial relationships that could be construed as a potential conflict of interest.

The authors declare that this study received funding from China Railway Fifth Bureau Group Mechanized Engineering Co. The funder had the following involvement in the study: data collection, study design, data collection and analysis, decision to publish, or preparation of the manuscript.

References

Ai, X., Pei, Z., Xu, K., Zhou, W., Wang, Y., Feng, D., et al. (2025). RAP agglomeration and partial blending of recycled hot mix asphalt: a literature review. *J. Road Eng.* 5, 230–243. doi:10.1016/j.jreng.2024.12.006

Akram, H., Hozayen, H. A., Abdelfatah, A., and Khodary, F. (2024). Fiber showdown: a comparative analysis of glass vs. polypropylene fibers in hot-mix asphalt fracture resistance. $Buildings\ 14\ (9),\ 2732.\ doi:10.3390/buildings\ 14092732$

Alfalah, A., Offenbacker, D., Ali, A., Mehta, Y., Elshaer, M., and Decarlo, C. (2021). Evaluating the impact of fiber type and dosage rate on laboratory performance of fiber-reinforced asphalt mixtures. *Constr. Build. Mater.* 310, 125217. doi:10.1016/j.conbuildmat.2021.125217

Algraiti, W., and Kavussi, A. (2023). The role of rejuvenating agents in cold recycled foam asphalt mixes. *Case Stud. Constr. Mater.* 19, e02515. doi:10.1016/j.cscm.2023.e02515

Anurag, K., Xiao, F., and Amirkhanian, S. N. (2009). Laboratory investigation of indirect tensile strength using roofing polyester waste fibers in hot mix asphalt. *Constr. Build. Mater.* 23 (5), 2035–2040. doi:10.1016/j.conbuildmat.2008.08.018

Bairgi, B. K., Mannan, U. A., and Tarefder, R. A. (2019). Influence of foaming on tribological and rheological characteristics of foamed asphalt. *Constr. Build. Mater.* 205, 186–195. doi:10.1016/j.conbuildmat.2019.02.009

Chen, Y., Pei, Z., Feng, D., and Yi, J. (2025). Environmental impact and comprehensive value assessment of epoxy-based binder for asphalt pavement recycling based on LCA and LCC. *Chem. Eng. J.* 511, 161973. doi:10.1016/j.cej.2025.161973

Fazilah, F. F. N. M., Masri, K. A., Al-Attab, A., and Jaya, R. P. (2025). "Performance Evaluation of Porous Asphalt Mixture Reinforced by Lignin Fiber," in IOP Conference Series: Earth and Environmental Science 1444 (1), 012026. doi:10.1088/1755-1315/1444/1/012026

Fei, M., Cai, Q., Wu, W., Yan, X., Zhao, H., Yu, K., et al. (2025). Surface modified slag fiber reinforced asphalt mixture: enhancement of pavement performance and field validation. *Case Stud. Constr. Mater.* 22, e04505. doi:10.1016/j.cscm.2025.e04505

Gong, X., Gu, H., Yan, H., Huang, X., Zhou, H., and Ma, J. (2025). Effect of aggregate roughness and film thickness on interfacial interaction of aggregate-asphaltaggregate films. *Constr. Build. Mater.* 486, 141984. doi:10.1016/j.conbuildmat.2025. 141984

He, G. P., and Wong, W. G. (2008). Effects of moisture on strength and permanent deformation of foamed asphalt mix incorporating RAP materials. *Constr. Build. Mater.* 22 (1), 30–40. doi:10.1016/j.conbuildmat.2006.06.033

Hu, Z., Zhang, J., Yu, X., Zhao, X., Lyu, L., Wang, Q., et al. (2024). Laboratory evaluation of cold recycled mixture with foamed waste oil-activated rubberized asphalt. *Transp. Res. Part D Transp. Environ.* 135, 104395. doi:10.1016/j.trd.2024.104395

Hui, Y., Men, G., Xiao, P., Tang, Q., Han, F., Kang, A., et al. (2022). Recent advances in basalt fiber reinforced asphalt mixture for pavement applications. *Materials* 15.19, 6826. doi:10.3390/ma15196826

Generative Al statement

The author(s) declare that no Generative AI was used in the creation of this manuscript.

Any alternative text (alt text) provided alongside figures in this article has been generated by Frontiers with the support of artificial intelligence and reasonable efforts have been made to ensure accuracy, including review by the authors wherever possible. If you identify any issues, please contact us

Publisher's note

All claims expressed in this article are solely those of the authors and do not necessarily represent those of their affiliated organizations, or those of the publisher, the editors and the reviewers. Any product that may be evaluated in this article, or claim that may be made by its manufacturer, is not guaranteed or endorsed by the publisher.

Kong, L., Lu, Z. F., He, Z. Y., Shen, Z., Xu, H., Yang, K., et al. (2022). Characterization of crack resistance mechanism of fiber modified emulsified asphalt cold recycling mixture based on acoustic emission parameters. *Constr. Build. Mater.* 327, 126939. doi:10.1016/j.conbuildmat.2022.126939

Li, Z., Hao, P., Liu, H., Xu, J., and Chen, Z. (2016). Investigation of early-stage strength for cold recycled asphalt mixture using foamed asphalt. *Constr. Build. Mater.* 127, 410–417. doi:10.1016/j.conbuildmat.2016.09.126

Li, Z., Hao, P., Liu, H., and Xu, J. (2019). Effect of cement on the strength and microcosmic characteristics of cold recycled mixtures using foamed asphalt. *J. Clean. Prod.* 230, 956–965. doi:10.1016/j.jclepro.2019.05.156

Li, Z., Li, K., Chen, W., Liu, W., Yin, Y., and Cong, P. (2022). Investigation on the characteristics and effect of plant fibers on the properties of asphalt binders. *Constr. Build. Mater.* 338, 127652. doi:10.1016/j.conbuildmat.2022.127652

Li, Q., Song, S., Wang, J., and Zhang, S. (2024). A review of the development of asphalt foaming technology. *J. Road Eng.* 4 (3), 334–347. doi:10.1016/j.jreng.2024.04.004

Lin, Q., Yan, G., and Yu, C. (2010). The analysis of the influence of fiber length distribution on the theoretical and additional unevenness of yarn. *Fibers Polym.* 11 (2), 266–270. doi:10.1007/s12221-010-0266-7

Liu, H., Li, Y., Li, J., Wang, F., Peng, L., Li, C., et al. (2023). Fiber-reinforced asphalt mixture design on anti-skid surfacing for field testing high-speed vehicles on pavements. *Materials* 16 (2), 549. doi:10.3390/ma16020549

Luo, D., Khater, A., Yue, Y., Abdelsalam, M., Zhang, Z., Li, Y., et al. (2019). The performance of asphalt mixtures modified with lignin fiber and glass fiber: a review. Constr. Build. Mater. 209, 377–387. doi:10.1016/j.conbuildmat.2019.

Meng, Y., Kong, W., Gou, C., Deng, S., Hu, Y., Chen, J., et al. (2023). A review on evaluation of crack resistance of asphalt mixture by semi-circular bending test. *J. Road Eng.* 3 (1), 87–97. doi:10.1016/j.jreng.2022.07.003

Nian, T., Wang, M., Ge, J., Guo, R., Li, P., and Song, J. (2024). Enhancing low-temperature crack resistance: a method for establishing meso-models and evaluating steel fiber-reinforced hot recycled asphalt mixtures. *Constr. Build. Mater.* 438, 137026. doi:10.1016/j.conbuildmat.2024.137026

Pang, Y., Li, H., Han, Z., Wu, P., and Lin, H. (2023). Performance evaluation of asphalt mixture reinforced by lignin and ceramic fiber. *J. Eng. Res.* 13, 1439–1448. doi:10.1016/j.jer.2023.10.035

Ren, D., Muhammad, Y., Chen, Y., Liu, Y., Mao, C., Xing, S., et al. (2022). Effect of PAN fiber with bionic layered surface structure generated *in situ* by fenton reaction on performance of SBS/RP asphalt binder. *Constr. Build. Mater.* 352, 129001. doi:10.1016/j.conbuildmat.2022.129001

Sengoz, B., and Agar, E. (2007). Effect of asphalt film thickness on the moisture sensitivity characteristics of hot-mix asphalt. *Build. Environ.* 42 (10), 3621–3628. doi:10.1016/j.buildenv.2006.10.006

Shi, C., Wang, J., Sun, S., Lv, D., Xu, L., and Zhang, S. (2023). Research on properties of basalt fiber-reinforced asphalt mastic. *Front. Mater.* 10, 1277634. doi:10.3389/fmats.2023.1277634

- Song, S., Li, Q., Wang, J., Shi, J., Wang, N., and Liu, T. (2024a). Evaluation of foaming performance for polymer modified and virgin asphalt binders. *Constr. Build. Mater.* 449, 138354. doi:10.1016/j.conbuildmat.2024.138354
- Song, S., Li, Q., Wang, J., Wang, N., Shang, J., and Zhang, S. (2024b). Utilization of thermoplastic resin as foamed asphalt modifier in cold recycled mixtures. *J. Clean. Prod.* 478, 143973. doi:10.1016/j.jclepro.2024.143973
- Wang, K., Qu, L., Tang, L., Hu, P., Wu, Q., Zhang, X., et al. (2024). Investigation on the performance of modified corn stalk fiber AC-13 asphalt mixture. *Coatings* 14 (4), 436. doi:10.3390/coatings14040436
- Wang, Y., Kang, A. H., Zhang, Y., Xiao, P., Wu, Z. G., and Gu, Q. L. (2025). Study on comprehensive performance evaluation and dynamic modulus model of fiber reinforced asphalt mixture. *Constr. Build. Mater.* 491, 142694. doi:10.1016/j.conbuildmat.2025.142694

- Wu, M. M., Li, R., Zhang, Y. Z., Fan, L., Lv, Y. C., and Wei, J. M. (2015). Stabilizing and reinforcing effects of different fibers on asphalt mortar performance. *Petroleum Sci.* 12 (1), 189–196. doi:10.1007/s12182-014-0011-8
- Wu, X., Easa, S., Kang, A., Xiao, P., Fan, Z., and Zheng, X. (2022). Performance evaluation of lignin-fibre reinforced asphalt mixture modified by anti-rutting agent. *Constr. Build. Mater.* 346, 128152. doi:10.1016/j.conbuildmat.2022. 128152
- Yue, Y., Abdelsalam, M., Khater, A., and Ghazy, M. (2022). A comparative life cycle assessment of asphalt mixtures modified with a novel composite of diatomite powder and lignin fiber. *Constr. Build. Mater.* 323, 126608. doi:10.1016/j.conbuildmat.2022.126608
- Zarei, M., Kordani, A. A., Khanjari, M., khajehzadeh, M., and Zahedi, M. (2022). Evaluation of fracture resistance of asphalt concrete involving calcium lignosulfonate and polyester fiber under freeze-thaw damage. *Theor. Appl. Fract. Mech.* 117, 103168. doi:10.1016/j.tafmec.2021. 103168